

Microwave-induced small size effect of $(\text{Ba}, \text{Sr})_3\text{MgSi}_2\text{O}_8:0.06\text{Eu}^{2+}, 0.1\text{Mn}^{2+}$ phosphor for 660 nm-featured bio-lighting

Li-sheng Cao^a, Qi-fei Lu^{a,b}, Ling-chang Wang^a, Jian Li^a, Jun Song^a,
Da-Jian Wang^{a,b,c,*}

^aInstitute of Materials Physics, Tianjin University of Technology, Tianjin 300384, PR China

^bTianjin Key Laboratory for Photoelectronic Materials and Devices, Tianjin 300384, PR China

^cKey Laboratory of Display Materials and Photoelectronic Devices (Tianjin University of Technology), Ministry of Education, Tianjin 300384, PR China

Received 6 February 2013; received in revised form 6 March 2013; accepted 10 March 2013

Available online 21 March 2013

Abstract

The 660 nm-featured $(\text{Ba}, \text{Sr})_3\text{MgSi}_2\text{O}_8:0.06\text{Eu}^{2+}, 0.1\text{Mn}^{2+}$ (AMS-EM) phosphor in violet for red/blue bio-lighting LEDs was prepared by 2.45 GHz microwave (MW) high temperature firing procedure. The phase-pure host phase, $(\text{Ba}, \text{Sr})_3\text{MgSi}_2\text{O}_8$, was formed to be responsible for simultaneous red band emission from Mn ion and blue band emission from Eu ion, while the formation of an impurity phase of Sr_2SiO_4 responsible for 505 nm-peaked green band emission for Eu ion was effectively suppressed owing to MW fast-heating procedure. Small sized and agglomeration-free phosphor particles were either observed, which was probably resulted from suppressing the grain growth in as-formed host particles, compared with conventional high-temp solid state (SS) reaction firing procedure. These results indicate that high-temp MW firing procedure is suitable for preparing this simultaneously red- and blue-emitting AMS-EM phosphor in the application of bio-lighting for plant cultivation.

© 2013 Elsevier Ltd and Techna Group S.r.l. All rights reserved.

Keywords: A. Microwave processing; C. Optical properties; E. Functional applications

1. Introduction

Application of microwave energy for ceramics processing is emerging as a novel and innovative technology [1–3] with many advantages over the other processing routes [4–10] such as reduction in processing cycle time resulting into substantial energy and cost savings, providing finer microstructures leading to improved properties [1].

Bio-lighting for plant cultivation was defined as a photosynthetic action spectrum consisting of a simultaneous 660 nm-red and 450 nm-blue emission [11–13]. For a potential bio-lighting phosphor of $\text{A}_3\text{MgSi}_2\text{O}_8:\text{Eu}^{2+}$ (A: Ba, Sr, Ca, AMS-E) or AMS: $\text{Eu}^{2+}, \text{Mn}^{2+}$ (AMS-EM), the high efficiency has been recognized for its blue, red or red–blue band emission since the 1960s [12–15], e.g.

the quantum efficiency for blue light is as high as 80% for AMS-E [16]. In particular, we defined a specific simultaneous emission in AMS-EM with red band for Mn^{2+} and blue band for Eu^{2+} upon near-ultraviolet (NUV) irradiation as a Photosynthetic Action Spectrum (PAS) for plant cultivation [12,17]. We have been exploring some effective means to scale up the preparation of the phosphors. In the conventional high-temperature SS synthesis procedure, there exist, however, some issues to be solved in particles size and host phase control. Although MW irradiation has been widely applied in aqueous or solvent solution processing of materials such as in organic synthesis [18], the high-temperature MW process needs to be optimized owing to great differences of dielectric properties of raw material with varied sizes and substantially inhomogeneous heating regime as subjected to MW field. However, only very limited data is available about the 660 nm-red emission of the $(\text{Ba}, \text{Sr})_3\text{MgSi}_2\text{O}_8:0.06\text{Eu}^{2+}, 0.1\text{Mn}^{2+}$ phosphor by MW firing processing procedure.

Herein, a 660 nm-peaked red and blue band emitting $(\text{Ba}, \text{Sr})_3\text{MgSi}_2\text{O}_8:0.06\text{Eu}^{2+}, 0.1\text{Mn}^{2+}$ phosphor was synthesized by high temperature microwave solid-state firing (MW).

*Corresponding author at: Institute of Materials Physics, Tianjin University of Technology, Tianjin 300384, PR China. Tel.: +86 22 6021 5386; fax: +86 22 6021 5553.

E-mail addresses: qifei_lu@163.com (Q.-f. Lu), djwang@tjut.edu.cn (D.-J. Wang).

Compared to the conventional Solid State Reaction (SS), a small particle size, particle uniformity and no agglomeration phenomenon of the fluorescent material are obtained. The reasons for the small particle size and host phase purity of MW-derived phosphors are to be discussed.

2. Experimental procedure

2.1. Sample preparation

Powder samples of an optimized nominal composition in $\text{Ba}_{1.3}\text{Sr}_{1.7}\text{MgSi}_2\text{O}_8:0.06\text{Eu}^{2+}, 0.1\text{Mn}^{2+}$ (BSMS-EM) were synthesized with high temperature MW and SS firing procedure. Chemicals such as BaCO_3 (AR), SrCO_3 (AR), nano- MgO (99.9%), SiO_2 (99.99%), Eu_2O_3 (99.99%), MnCO_3 (99.9%) and a small amount of flux and NH_4Cl (about 10 wt %) were used as raw materials. The properly-blended mixture was fired under N_2 92– H_2 8 vol% atmosphere for 2 h at 900 °C, 1000 °C, 1100 °C, 1200 °C and 1300 °C in a MW furnace (1.5 KW, 2.45 GHz, max. temp. 1600 °C, HAMiLab-V1500, Synotherm Ltd., China) by MW and a counterpart sample was fired for 2 h in a tube furnace (4 KW, max. temp. 1600 °C, Hefei Kejin Materials Tech. Co. Ltd., China) by SS at 1300 °C.

2.2. Characterization

As-prepared samples were investigated by X-ray power diffraction (XRD) with a diffractometer (Rigaku D/max-2500/pc, Japan). The photoluminescence (PL) and photoluminescence of excitation (PLE) spectra of samples were recorded on a fluorescence spectrometer equipped with a xenon light source (Hitachi F-4600, Japan). The diffuse-reflectance spectra (DRS) were recorded by UV–Visible spectrometer (TU-1901, China) with a 60-mm diameter integration sphere. Particle size analysis was carried out using a BT-9300H laser scattering particle size analyzer. The surface morphology and the size of samples were observed with field emission-scanning microscopy (FE-SEM; Model S-4800, Hitachi Japan). All measurements were carried out at room temperature.

3. Results and discussion

3.1. Photoluminescence properties

Fig. 1 shows the dependence of photoluminescence (PL) and PL of excitation (PLE) spectra of BSMS-EM on the holding temperature as fired by MW and SS. PLE spectrum (Fig. 1a) shows that all the samples are excitable in the wavelength range from UV to NUV, while the PL spectrum (Fig. 1b) exhibits a dual peak band emission consisting of a blue emission band peaked at 432 nm from 4f to 5d transition of Eu^{2+} and a red band emission peaked at 660 nm from the 4T to 6A transition of $3d^5$ energy level of Mn^{2+} in the host of AMS-EM. It has been well verified that the excitation energy of Mn ion for 660 nm-peaked red band emission is transferred from Eu^{2+} through lattice vibration [13]. In general, the

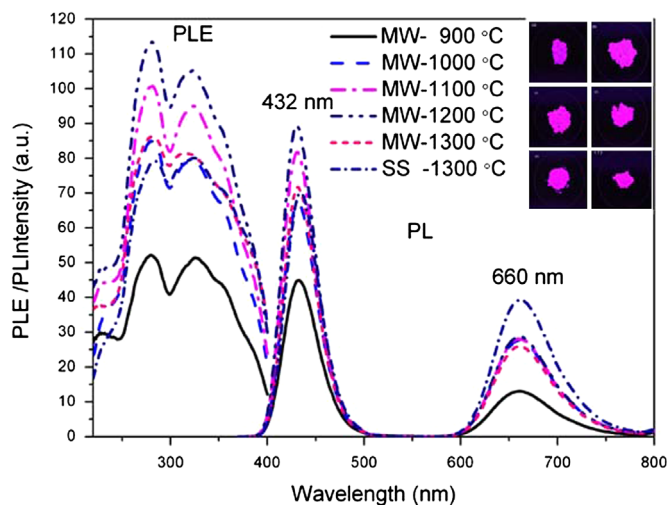


Fig. 1. Photoluminescence of excitation (PLE) spectrum monitored at 432 nm and photoluminescence (PL) spectrum excited at 350 nm of the $\text{Ba}_{1.14}\text{Sr}_{1.7}\text{MgSi}_2\text{O}_8:0.06\text{Eu}^{2+}, 0.1\text{Mn}^{2+}$ (BSMS-EM) samples prepared by MW and SS, respectively. The inset represents the photographs of $\text{Ba}_{1.14}\text{Sr}_{1.7}\text{MgSi}_2\text{O}_8:0.06\text{Eu}^{2+}, 0.1\text{Mn}^{2+}$ phosphors under 365 nm excitation.

intensity of PL increases with increasing MW holding temperature from 900 °C to 1000 °C.

3.2. Mechanism of microwave firing

In general, the raw materials and the inorganic host of this $(\text{Ba}, \text{Sr})_3\text{MgSi}_2\text{O}_8: 0.06\text{Eu}^{2+}, 0.1\text{Mn}^{2+}$ phosphor are transparent to the microwave energy. Some auxiliary heating parts such as SiC or ZrO_2 with higher dielectric loss factor were used in the experiments. With the increasing temperature of heated materials such as ceramic materials, the dielectric properties of heated materials are believed to be increased [19] to achieve more homogeneous volume heating of materials finally [20]. Under the properly-optimized MW parameters and implantation of auxiliary heating parts, the faster heating of MW in non-equilibrium suppressed the formation of the impurity phase of $(\text{Ba}, \text{Sr})_2\text{Si}_2\text{O}_4$ that frequently coexists with the phase of $(\text{Ba}, \text{Sr})_3\text{MgSi}_2\text{O}_8$ host in the conventional heating. This faster heating procedure also leads to a small size effect of phosphor particles as interpreted in Section 3.5.

3.3. Diffuse reflection spectra

Fig. 2 shows the diffuse reflection spectra (DRS) of as-fired BSMS-Eu, Mn samples. The absorption of incident photonic energy by Mn^{2+} is, however, very weak in most host lattices due to its spin and parity forbidden d–d transitions. An efficient sensitizer such as Eu is generally needed as a dopant pair to promote the green–red emission of Mn ion. It was observed from Fig. 2 that there exists an absorption band peaked at around 250 nm corresponding to the valence-to-conduction band transitions of the BSMS host lattice. In the Eu^{2+} and Mn^{2+} co-doped BSMS, two absorption bands are in the wavelength range from 200 to 430 nm, which can be ascribed to the charge transfer band absorption and the

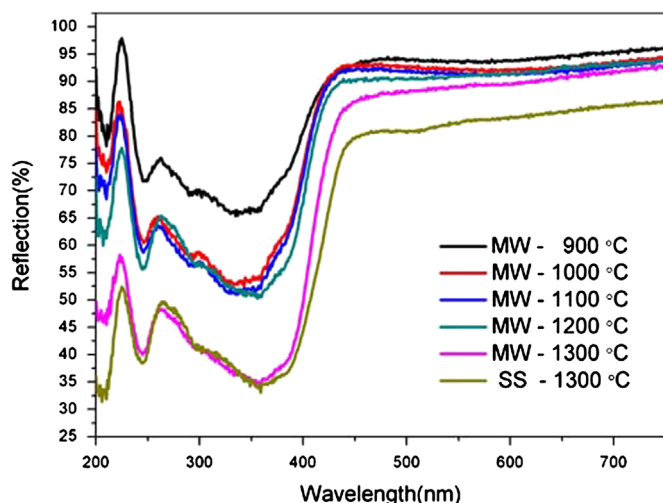


Fig. 2. Diffuse reflection spectra of $\text{Ba}_{1.14}\text{Sr}_{1.7}\text{MgSi}_2\text{O}_8:0.06\text{Eu}^{2+}, 0.1\text{Mn}^{2+}$ (BSMS-EM) samples.

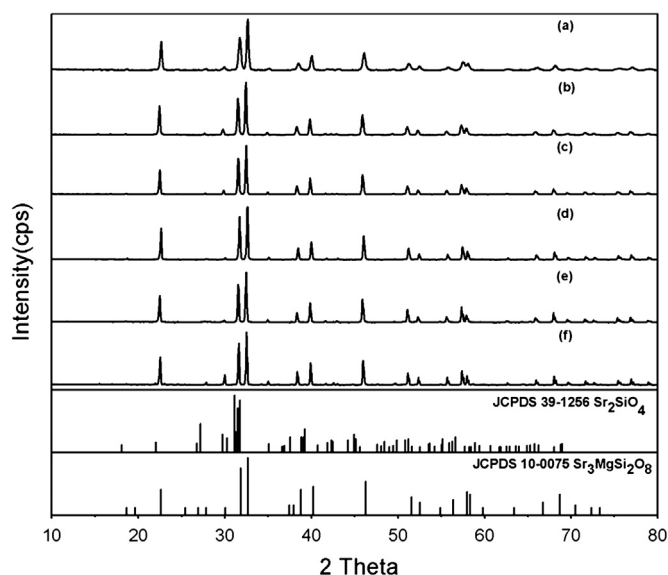


Fig. 3. The X-ray diffraction (XRD) patterns of $\text{Ba}_{1.14}\text{Sr}_{1.7}\text{MgSi}_2\text{O}_8:0.06\text{Eu}^{2+}, 0.1\text{Mn}^{2+}$ samples as fired at different temperatures by MW at (a) 900 °C; (b) 1000 °C; (c) 1100 °C; (d) 1200 °C; (e) 1300 °C and SS at (f) 1300 °C.

transition absorption from the ground-state $4f^7$ of Eu^{2+} to its excited state $4f^65d^1$, respectively. No distinct transition absorption can be observed for Mn ion, indirectly confirming an occurrence of effective energy transfer between Eu and Mn ions via the lattice. These results are in good agreement with the PLE spectra, as shown in Fig. 2.

3.4. Structure

Fig. 3 shows the X-ray diffraction (XRD) patterns of typical $\text{Ba}_{1.14}\text{Sr}_{1.7}\text{MgSi}_2\text{O}_8:0.06\text{Eu}^{2+}, 0.1\text{Mn}^{2+}$ samples as fired at different temperatures by MW. In this Ba–Sr solid solution system of host phase, no trace phase of $\text{Ba}_3\text{MgSi}_2\text{O}_8$ was identified from the measured diffraction patterns. The

crystallographic frame agrees well with that of $\text{Sr}_3\text{MgSi}_2\text{O}_8$ (JCPDS 10-0075), indicating a partial substitution of Ba at Sr lattice sites in a solid solution form for the above-mentioned composition.

More importantly, we observed the size effect of phosphor particles versus MW power as fired with MW procedure. As shown in Fig. 4, the particle exhibits a D_{50} value of around 8–10 μm in a uniform size distribution from 900 to 1200 W for MW-derived particles while that for SS-derived particles is greater than ten micrometers. This difference can also be demonstrated by typical SEM images, as shown in the photograph inset in Fig. 4(b) and (c). The SEM image of phosphors prepared by MW firing procedure exhibits a smooth surface for the majority of particles than those by SS.

3.5. Size and morphology analyses

The size effect of MW firing procedure probably reveals the interaction between MW magnetic field relevant to the non-thermal effect and crystalline solids during the process. Boosk et al. [21] presented a non-thermal mechanism for MW-enhanced surface diffusion in annealing nano-porous aluminum oxide membranes by 2.45 GHz microwave radiation. As Boosk et al. explained, the reduction of activation for diffusion and overall faster kinetics might be responsible for the suppression of grain growth during MW firing process. Similarly, Wada et al. [22] observed that size of nickel metal particle prepared by MW firing process was ten times smaller than that of the particle prepared by SS firing process as obtained by Hegde et al. [23]. Wada considered MW irradiation may cause different nucleation and growth patterns of Ni metal particles due to the high dielectric loss properties of Ni $(\text{OH})_2$ and ethylene glycol [22]. Then Nakayama [24] reported that the particle size of LiMn_2O_4 prepared by MW irradiation is smaller than the reference sample prepared by electric furnace. Nakayama thought that the growth of grain size due to sintering effect does not occur in the reaction, and fine particles of LiMn_2O_4 are obtained, while Mark P. McNeal [25] shows the potential to tune the MW properties of ferroelectrics through control of grain/particle size and the domain state. We also prefer to the mechanism of MW non-thermal effects in this MW processing $(\text{Ba}, \text{Sr})_3\text{MgSi}_2\text{O}_8:0.06\text{Eu}^{2+}, 0.1\text{Mn}^{2+}$ (BSMS-EM), namely a suppression of the diffusion and grain growth of particles owing to faster heating procedure.

4. Conclusions

The 660 nm-featured band emission phosphor of $(\text{Ba}, \text{Sr})_3\text{MgSi}_2\text{O}_8:0.06\text{Eu}^{2+}, 0.1\text{Mn}^{2+}$ (BSMS-EM) was achieved by MW procedure for the purpose of bio-lighting in plant cultivation. The desired phosphor was obtained in a pure host phase by effectively suppressing a green-emitting impurity phase of Sr_2SiO_4 but with a smaller particle size and a smoother surface by MW than by SS, affected by microwave magnetic field during firing process, indicating a realization to prepare the multi-component, small sized phosphor materials efficiently by MW procedure.

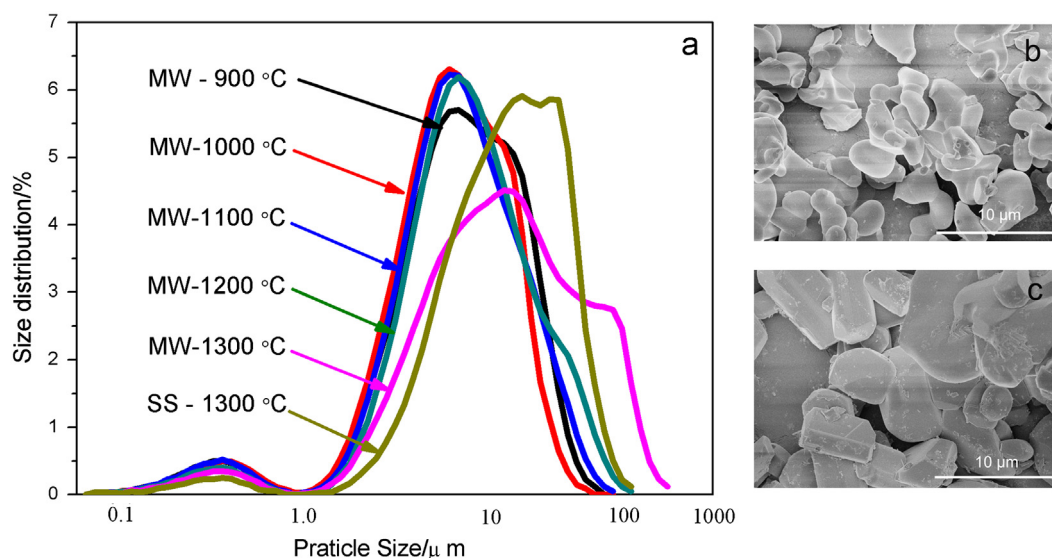


Fig. 4. Particle size (a) and morphology of BSMS-EM samples as fired by MW (b) and SS (c).

Acknowledgments

This work was financially supported by the National Natural Science Foundation of China under Grant nos. 21076161, 50802062, and 50872091 and Tianjin Key Discipline of Materials Physics and Chemistry under Grant no. 10SYSYJC28100.

References

- [1] D. Agrawal, Latest global developments in microwave materials processing, *Materials Research Innovations* 14 (1) (2010) 3–8.
- [2] H.Y. Chen, M.H. Weng, S.J. Chang, R.Y. Yang, Preparation of $\text{Sr}_2\text{SiO}_4:\text{Eu}^{3+}$ phosphors by microwave-assisted sintering and their luminescent properties, *Ceram International* 38 (1) (2012) 125–130.
- [3] S. Das, A.K. Mukhopadhyay, S. Datta, D. Basu, Prospects of microwave processing: an overview, *Materials Science and Engineering: B* 32 (1) (2009) 1–13.
- [4] L.H. Zhang, H.Y. Zhong, X.P. Li, L.H. Cheng, L. Yao, J.S. Sun, J.S. Zhang, R.N. Hua, B.J. Chen, Solid state reaction synthesis and photoluminescence properties of Dy^{3+} doped $\text{NaGd}(\text{MoO}_4)_2$ phosphor, *Ceram International* 38 (6) (2012) 4737–4743.
- [5] M. Zeng, Y.J. Ma, Y.H. Wang, C.H. Pei, The effect of precipitant on co-precipitation synthesis of yttrium aluminum garnet powders, *Ceram International* 38 (8) (2012) 6951–6956.
- [6] M. Misevicius, O. Scit, I. Grigoraviciute-Puroniene, G. Degutis, I. Bogdanoviciene, A. Kareiva, Sol-gel synthesis and investigation of un-doped and Ce-doped strontium aluminates, *Ceram International* 38 (7) (2012) 5915–5924.
- [7] K.S. Hwang, S. Hwangbo, J.T. Kim, Sol-gel synthesis of red-emitting LiEuW_2O_8 powder as a near-ultraviolet convertible phosphor, *Ceram International* 35 (6) (2009) 2517–2519.
- [8] H.J. Lee, S.K. Hong, D.S. Jung, S.H. Ju, H.Y. Koo, Y.C. Kang, The characteristics of X1 type $\text{Y}_2\text{SiO}_5:\text{Tb}$ phosphor particles prepared by high temperature spray pyrolysis, *Ceram International* 32 (8) (2006) 865–870.
- [9] K.H. Hsu, K.S. Chen, Photoluminescence of ZnGa_2O_4 phosphor prepared by a microencapsulation method, *Ceram Int* 26 (5) (2000) 469–473.
- [10] J.H. Chung, J.H. Ryu, Photoluminescence and LED application of beta- $\text{SiAlON}:\text{Eu}^{2+}$ green phosphor, *Ceram International* 38 (6) (2012) 4601–4606.
- [11] R. Emerson, R. Chalmers, C. Cederstrand, Some factors influencing the long-wave limit of photosynthesis, *Proceedings of the National Academy of Sciences of the United States of America* 43 (1) (1957) 133.
- [12] L. Ma, D.J. Wang, Z.Y. Mao, Q.F. Lu, Z.H. Yuan, Investigation of Eu–Mn energy transfer in $\text{A}_3\text{MgSi}_2\text{O}_8:\text{Eu}^{2+}, \text{Mn}^{2+}$ ($\text{A}=\text{Ca}, \text{Sr}, \text{Ba}$) for light-emitting diodes for plant cultivation, *Applied Physics Letters* 93 (14) (2008) 144101.
- [13] T.L. Barry, Equilibria and Eu^{2+} luminescence of subsolidus phases bounded by $\text{Ba}_3\text{MgSi}_2\text{O}_8$, $\text{Sr}_3\text{MgSi}_2\text{O}_8$ and $\text{Ca}_3\text{MgSi}_2\text{O}_8$, *Journal of The Electrochemical Society: Solid State Science* 115 (1968) 733–738.
- [14] Y. Yonesaki, T. Takei, N. Kumada, N. Kinomura, Sensitized red luminescence from Ce^{3+} , Mn^{2+} -doped glaserite-type alkaline-earth silicates, *Journal of Solid State Chemistry* 183 (6) (2010) 1303–1308.
- [15] W.B. Im, Y.I. Kim, H.S. Yoo, D.Y. Jeon, Luminescent and Structural properties of $(\text{Sr}_{1-x}, \text{Ba}_x)_3\text{MgSi}_2\text{O}_8:\text{Eu}^{2+}$: Effects of Ba Content on the Eu^{2+} Site preference for Thermal Stability, *Inorganic Chemistry* 48 (2) (2009) 557–564.
- [16] G. Blasse, W.L. Wanmaker, J.W. Vrugt, A. ter, Bril, Fluorescence of Eu^{2+} activated silicates, *Philips Research Reports* 23 (1968) 189–200.
- [17] L. Ma, D.J. Wang, H.M. Zhang, T.C. Gu, Z.H. Yuan, The origin of 505 nm-peaked photoluminescence from $\text{Ba}_3\text{MgSi}_2\text{O}_8:\text{Eu}^{2+}, \text{Mn}^{2+}$ phosphor for white-light-emitting diodes, *Electrochemical and Solid State Letters* 11 (2) (2008) E1–E4.
- [18] I. Bilecka, M. Niederberger, Microwave chemistry for inorganic nano-materials synthesis, *Nanoscale* 2 (8) (2010) 1358–1374.
- [19] W.H. Sutton, Microwave processing of ceramic materials, *American Ceramic Society Bulletin* 68 (2) (1989) 376–386.
- [20] A. Birkel, K.A. Denault, N.C. George, C.E. Doll, B. Héry, A. A. Mikhailovsky, C.S. Birkel, B.C. Hong, R. Seshadri, Rapid microwave preparation of highly efficient Ce^{3+} -substituted garnet phosphors for solid state white lighting, *Chemistry of Materials* 24 (6) (2012) 1198–1204.
- [21] C.J. Bonifas, A. Marconnet, J. Perry, J.H. Booske, R.F. Cooper, Microwave-induced mass transport enhancement in nano-porous aluminum oxide membranes, *Journal of Microwave Power and Electromagnetic Energy* 42 (1) (2008) 13.
- [22] Y. Wada, H. Kuramoto, T. Sakata, H. Mori, T. Sumida, T. Kitamura, S. Yanagida, Preparation of nano-sized metal particles by microwave irradiation, *Chemistry Letters* 7 (1999) 607–608.
- [23] M. Hegde, D. Larcher, L. Dupont, B. Beaudoin, K. Tekaia-Elhsissen, J.-M. Tarascon, Synthesis and chemical reactivity of polyol prepared monodisperse nickel powders, *Solid State Ionics* 93 (1) (1996) 33–50.
- [24] M. Nakayama, K. Watanabe, H. Ikuta, Y. Uchimoto, M. Wakihara, Grain size control of LiMn_2O_4 cathode material using microwave synthesis method, *Solid State Ionics* 164 (1–2) (2003) 35–42.
- [25] M.P. McNeal, S.J. Jang, R.E. Newnham, The effect of grain and particle size on the microwave properties of barium titanate (BaTiO_3), *Journal of Applied Physics* 83 (6) (1998) 3288–3297.